Nanoscale Advances

ROYAL SOCIETY OF CHEMISTRY

MINIREVIEW

View Article Online
View Journal | View Issue

Cite this: *Nanoscale Adv.*, 2021, **3**, 4907

Sound methods for the synthesis of nanoparticles from biological molecules

Sukhvir Kaur Bhangu, [a] Anshul Baral, [b] Haiyan Zhu, [b] Muthupandian Ashokkumar *[b] and Francesca Cavalieri *[ac]

Received 28th June 2021
Accepted 19th July 2021

DOI: 10.1039/d1na00496d

rsc.li/nanoscale-advances

The development of simple, green, reproducible, and scalable approaches for synthesizing nanoparticles from biomolecules is important to advance nanomaterials towards therapeutic applications. Microreactors generated by high frequency ultrasound provide a one pot-platform to alter the physiochemical properties and stability of various types of biomolecules to ultimately generate multifunctional nanoparticles with controlled size and morphology. Herein, recent advancements in the field of nanoparticles fabrication from amino acids, phenolics, peptides and proteins using both high and low frequency ultrasound are reviewed. In particular, the sound driven self-assembly of biomolecules into nanoparticles by using high frequency ultrasound, as an emerging and innovative approach, is discussed in detail.

1. Introduction

Nanoparticles originating from natural biomolecules (*e.g.*, amino acids, proteins, peptides, polyphenols) have been attracting substantial attention because of their degradability, limited toxicity, and bio-functional properties. Nanoparticles derived from biomolecules can themselves act as therapeutic agents or be employed as carriers for delivery of drugs and contrast agents.[1] The physicochemical characteristics of the nanoparticles including the size, shape, chemical composition, stability, surface energy and degradability play a pivotal role in determining the bioactivity and toxicity of the engineered nanoparticles.[2] Particularly, numerous studies on the therapeutic use of nanoparticles have shown that the cellular interactions, cellular uptake efficiency and mechanism, the

[a]*School of Science, RMIT University, Melbourne, VIC 3000, Australia. E-mail: francesca.cavalieri@rmit.edu.au*

[b]*School of Chemistry, University of Melbourne, VIC 3010, Australia. E-mail: masho@unimelb.edu.au*

[c]*Dipartimento di Scienze e Tecnologie Chimiche, Universita' di Roma "Tor Vergata", Via della Ricerca Scientifica 1, 00133, Rome, Italy*

Sukhvir Kaur Bhangu is a post-doctoral researcher at RMIT University, Australia. She received her PhD in 2019 from University of Melbourne, Australia in Chemistry and developed ultrasonic method for modification and self-assembly of biomolecules and drug molecules. Her research interests are fabrication of new generation of nanostructures from various biomolecules for cancer therapy, gene therapy and single-molecule localization microscopy.

Anshul Baral is currently doing his PhD in Chemistry at the University of Melbourne, Australia. Prior to joining the University of Melbourne, he worked as Project Officer at the Rubber Technology Centre at Indian Institute of Technology Kharagpur (India) and developed the technique to measure penetration/stubble resistance of rubber vulcanizates. He did his masters project on graphene-based membranes for purification and catalytic applications at the Institute for Physical Chemistry and Polymer Physics at the Leibniz-Institut für Polymerforschung Dresden (Germany). His current research interests are focused on exploring the fundamentals of ultrasound techniques for fabricating bio-functional and metallic nanostructures for biomedical and catalytic applications.

intracellular trafficking, *in vivo* biodistribution and clearance are strictly dictated by their chemical and structural features.[2–5]

Hence, innovative methods to design nanoparticles with controlled and reproducible chemical and structural properties are in great demand. The most common building blocks for the fabrication of nanoparticles include-metals, inorganic materials, synthetic polymers and biopolymers.[6–9] The strategies which are usually utilised for the synthesis of organic and inorganic nanoparticles include sol–gel reactions, mechanical milling, microemulsion polymerization, self-assembly, inorganic templates, chemical vapor deposition and biogenic synthesis.[10] Despite the advantages offered by these methods, they typically require multiple starting chemical components, initiators, crosslinkers, organic solvents, and laborious manufacturing procedures. Therefore, the development of green, and cost-effective methods for engineering nanoparticles composed entirely of biological molecules, without resorting to synthetic agents and organic solvents, could be a viable strategy to improve the manufacturing of the new generation of nanoparticles. Ultrasound (sound waves beyond the frequency that can be detected by human ear), as an eco-friendly technology, has a great potential for the nanofabrication of organic, inorganic and organometallic materials.[11–14] For instance, in the last decade ultrasound-based techniques have been used for the preparation of microcapsules and microbubbles stabilized by crosslinked proteins shells[15,16] to obtain biodegradable acoustic contrast agents and encapsulation of micronutrients, as well as metal and oxide nanoparticles[13,17] which were employed for catalytic and drug delivery applications.

The driving force behind all sonochemical processes is the acoustic cavitation. When ultrasound energy is transmitted to a liquid medium it leads to the formation, growth and collapse of cavitation bubbles. This phenomenon, referred to as acoustic cavitation, produces both physical and chemical effects.[18] Microbubbles grow to a resonance size range and collapse near adiabatically generating extreme and transient (microsecond timescale) temperature (~5000 K) and pressure (>100 atm) conditions within the bubbles. The violent collapse of acoustic cavitation bubbles leads to the homolysis of water molecules to form primary hydrogen and hydroxyl radicals, when ultrasound is applied in aqueous media.[18,19] Besides, the collapse of acoustic cavitation bubbles is usually accompanied by shock waves, micro-streams, and microjets, which have their usage in improving mass transfer and reaction kinetics.[20] The physicochemical effects generated by an ultrasound, *i.e.*, shear stress, oxidant and reducing environments, can be exploited for the fabrication of nanostructured materials. The extent of these physical and chemical effects can be controlled by fine tuning the ultrasonic parameters including frequency, power and sonication time.[21] Numerous studies have shown that the number and size of cavitation bubbles generated depend on the ultrasound frequency.[21] Typically, the size of acoustic bubbles is inversely proportional to frequency, and the radical yield rises with the surge in frequency, reaching an optimal level between

Haiyan Zhu obtained her B.S. degree in Applied Chemistry from University of Shanghai for Science and Technology in 2016. Then, she joined the University of Melbourne and received her M.S. degree in Chemistry in 2018. She was awarded "Melbourne Research Scholarship" for pursuing further research study. Now, she is currently doing her PhD in the University of Melbourne. Her research focuses on fabrication of bio-functional nanostructures by using eco-friendly ultrasonic technique and their applications in nutrients and drug delivery fields.

Professor Muthupandian Ashokkumar (Ashok) is a Physical Chemist who specializes in Sonochemistry and is a senior academic staff member of the School of Chemistry, University of Melbourne. He is currently the Assistant Deputy Vice-Chancellor International at the University of Melbourne. Ashok is a renowned sonochemist, with about 25 years of experience in this field, and has developed a number of novel techniques to characterize acoustic cavitation bubbles and has made major contributions of applied sonochemistry to the Materials, Food and Dairy industry.

Dr Francesca Cavalieri received her Laurea degree, 'maxima cum laude,' in Industrial Chemistry in 1995 from the University of Rome La Sapienza. She completed her PhD in Chemistry at the University of Melbourne in 2014. She has been a tenured Ag/Professor in Polymer Science in the Department of Chemistry, at the University of Rome 'Tor Vergata' since 2002. She was awarded the ARC Future Fellowship at the University of Melbourne in 2015. She is currently appointed as Vice Chancellor Senior Fellow at RMIT University, Australia. Dr Cavalieri has an expertise in the synthesis and characterization of nanostructured materials based on biomacromolecules (polysaccharides, proteins, nucleic acids).

200 kHz and 800 kHz.[21–25] The low frequency ultrasound (20 kHz) primarily produces strong shear forces and low radical yields and it has found applications in the preparation of nano-microemulsions, synthesis of polymers,[26,27] and micro-nanocapsules.[15,28] Overall ultrasound generates microreactors and reactive liquid–gas interfaces that can be exploited to engineer new nanomaterials with controlled size and morphology by tuning the ultrasonic processing parameters.[29,30]

2. Ultrasound-driven nanostructures from biomolecules

In this minireview, we will report the recent studies on the ultrasound mediated self-assembly and oxidative coupling of amino acids specifically-tyrosine derivatives, tryptophan, phenylalanine; phenolics – naturally occurring polyphenolic molecules; short synthetic peptides and various natural proteins – soy peptides, quinoa protein, to highlight the potential of sound-based methods as innovative and sustainable approaches for the synthesis of nanoparticles from biological molecules. The review also provides a discussion on the detailed mechanistic aspects involved in the formation of such nanomaterials and their applications in biomedical and food fields.

2.1 Ultrasound-driven oxidation and self-assembly of amino acids into nanoparticles

Acoustic cavitation in aqueous solutions containing small aromatic amphiphilic molecules can cause a series of reactions, without the addition of any external reagents, and lead to the generation of reactive radical species to initiate hydroxylation, oligomerization, and self-assembling processes. These processes can take place in bulk water phase or at air–liquid interface to form high molecular weight products, *i.e.*, dimers, oligomers. Cavalieri[31] and co-workers reported for the first time the mechanism involved in the oxidative coupling and self-assembly of tyrosine derivative molecule – *N*-benzoyl-L-tyrosine ethyl ester (BTEE). During the application of ultrasound (high frequency ultrasound in the range of 0.35–1 MHz), gas–liquid interface of the oscillating acoustic cavitation microbubbles acts as a reactive and catalytic binding site for the coupling of amphiphilic surface-active aromatic moieties into oligomers.[31] In analogy with enzymes and inorganic catalysts, the catalytic coupling of phenoxyl radicals at the bubble–solution interface implies a mechanism whereby the aromatic rings of tyrosyl radicals approach each other at the liquid–gas interface prior to their oxidation and coupling (Fig. 1a). Furthermore, the obtained oligomers can form well-defined nanoparticles upon self-assembly triggered by ultrasound (Fig. 1b).

In terms of overall mechanism, surface active monomer molecules are initially adsorbed at the interface of the cavitation bubbles. The aromatic amino acid is then attacked by OH radicals provided by bubble collapse to form phenoxy radicals and hydroxylated monomers and dimers. The continuation of this process can lead to the formation of other high molecular weight oligomers. Finally, these oligomeric species when adsorbed on cavitation bubble surface can self-assemble through intermolecular π–π interactions to form uniform nanoparticles (Fig. 1b) upon bubble collapse. The phenomenon can be also employed to crosslink tyrosine-bearing proteins such as albumin to form protein-based nanoparticles. The tyrosine-based nanoparticles possess remarkable optical properties emitting blue, green and red light (Fig. 1b and c) because of the chemical coupling reactions and π–π stacking interactions between oligomers and enhanced antioxidant activity due to the presence of high degree of hydroxylation. This seminal work paved the way for the engineering of phenolics and amino acid-based nanostructured materials using the one pot, reagentless and facile ultrasonic approach.

The sound driven oxidation and self-assembly of sono-responsive aromatic amino acids like phenylalanine and tryptophan was recently reported to fabricate well-defined nanoparticles.[32,33] The method involves the hydroxylation and coupling of aromatic amino acids to form dimeric species (Fig. 2a), which further self-assembled by π–π interaction and H-bonding into spherical and uniform nanoparticles. The size of phenylalanine-based nanoparticles synthesised at 490 kHz can be tuned from 607 ± 88 nm 190 ± 50 nm as sonication power levels were increased from 2 W cm^{-2} to 6 W cm^{-2}, respectively (Fig. 2b). The average diameter and ζ-potential of tryptophan nanoparticles was 230 nm ± 50 nm and −26 ± 7 mV respectively. Similarly, hybrid nanoparticles were obtained when a mixture of phenylalanine and tryptophan was sonicated (Fig. 2a). The formation of homodimers and heterodimers of phenylalanine and tryptophan was confirmed using mass spectrometry.

The potential applications of tryptophan nanoparticles as drug delivery systems were investigated by studying the intracellular trafficking and drug release. These nanoparticles were promptly internalized in MDA-MB-231 cells, trafficked from early to late endosomes, released into the cytosol by escaping the endosomes and dissolved in the neutral cytosolic environment without causing any cytotoxicity (Fig. 2c). The nanoparticles were internalised through micropinocytosis and escape of nanoparticles from late endosomes occurred between 5 h and 8 h. Fig. 2c shows that nanoparticles (green) were colocalised (yellow) with early and late endosomes (red) after 2 h incubation, whereas negligible colocalization with the organelles was found after 8 h incubation. This was attributed to the ability of nanoparticles to escape the late endosomal compartments by the proton sponge effect due to their intrinsic buffering capacity in the pH range from 7 to 5. The synthesised amino acid-based nanoparticles showed superior radical scavenging activity within only 2 min of incubation with DPPH radical when compared to the parent amino acids, and excellent intrinsic fluorescent properties (Fig. 2d). Furthermore, the sono-assembled tryptophan nanoparticles showed high loading of doxorubicin (DOX-a chemotherapeutic drug), mediated by electrostatic and hydrophobic interactions, and cytotoxicity (Fig. 2e) comparable to the free drug in human breast cancer cell line (MDA-MB-231 cells). The drug intracellular release and

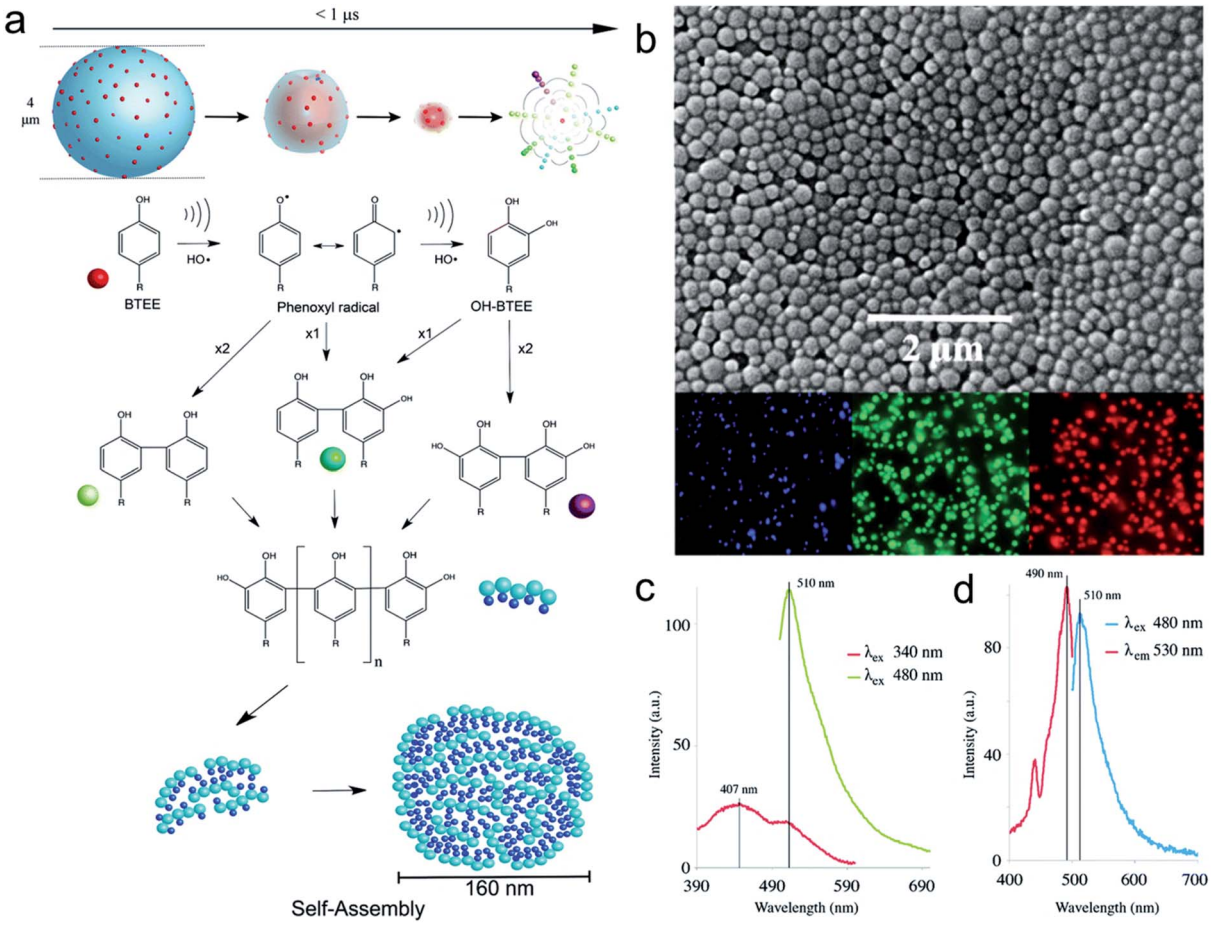

Fig. 1 (a) Scheme representing ultrasound mediated coupling of aromatic moieties into hydroxylated and high molecular weight species and their self-assembly to form nanoparticles. The time scale for bubble collapse is based on single bubble dynamics calculations. (b) SEM and fluorescent microscopy images of BTEE nanoparticles (c) Fluorescence emission spectra of BTEE nanoparticles at excitation wavelength 340 nm and 480 nm (d) Fluorescence excitation and emission spectra of BTEE nanoparticles at emission wavelength 530 nm and excitation wavelength 480 nm.[31] (Reproduced from ref. 31 with permission from The Royal Society of Chemistry.)

localization in the nucleus was tracked over time by confocal microscopy.

Interestingly in this study,[33] tryptophan was used as a model molecule to unveil for the first time, how acoustic cavitation is involved in the dissipative self-assembly process to form supramolecular nanoaggregates. It was shown that the nanoparticles were formed well below the critical aggregation concentration of tryptophan dimers and that a transient energy input given by ultrasound can push the aromatic dimers from global minimum to a high-energy state and provide transient liquid–air interface where the self-assembly of biomolecules into nanoaggregates can take place, on bubble collapse (Fig. 3a – Gibbs free energy landscape of dissipative self-assembly of tryptophan dimers nanoparticles).

The general scheme for ultrasound driven dissipative self-assembly of tryptophan dimers to nanoparticles is provided in Fig. 3b which suggests that the cavitation bubble can act as a fuel and template for adsorption of tryptophan dimers. It was postulated that the local high concentration of tryptophan dimers on the air–liquid interface (Fig. 3b-step 1) facilitates the nanoaggregation upon bubble collapse (step 2 and 3). The nanoparticles can dissipate energy upon increasing the pH by disassembly into the building blocks (step 3), and the acoustic energy can refuel the dissipative self-assembly of tryptophan dimers, below the cac, to reform nanoparticles (step 4).

Moreover, molecular dynamics studies also supported the hypothesis that collapse of bubbles can induce the formation of nanoaggregates through different intermolecular interactions such as- ionic interactions between the charged carboxyl and amine groups (Fig. 3c), the stabilization of π–π interactions due to aromatic moieties (Fig. 3d) and hydrogen bonding in which the aromatic ring act as acceptor (Fig. 3e). These findings were supported experimentally by studying the fluorescence properties of the nanoparticles in a wide spectral range. These peculiar spectral features of these nanoparticles were exploited to track their intracellular trafficking and disassembling.

2.2 Ultrasound-driven transformation and self-assembly of phenolic molecules

Bhangu *et al.*[34] confirmed the general concept of ultrasound assisted self-assembly of phenol-like molecules by obtaining

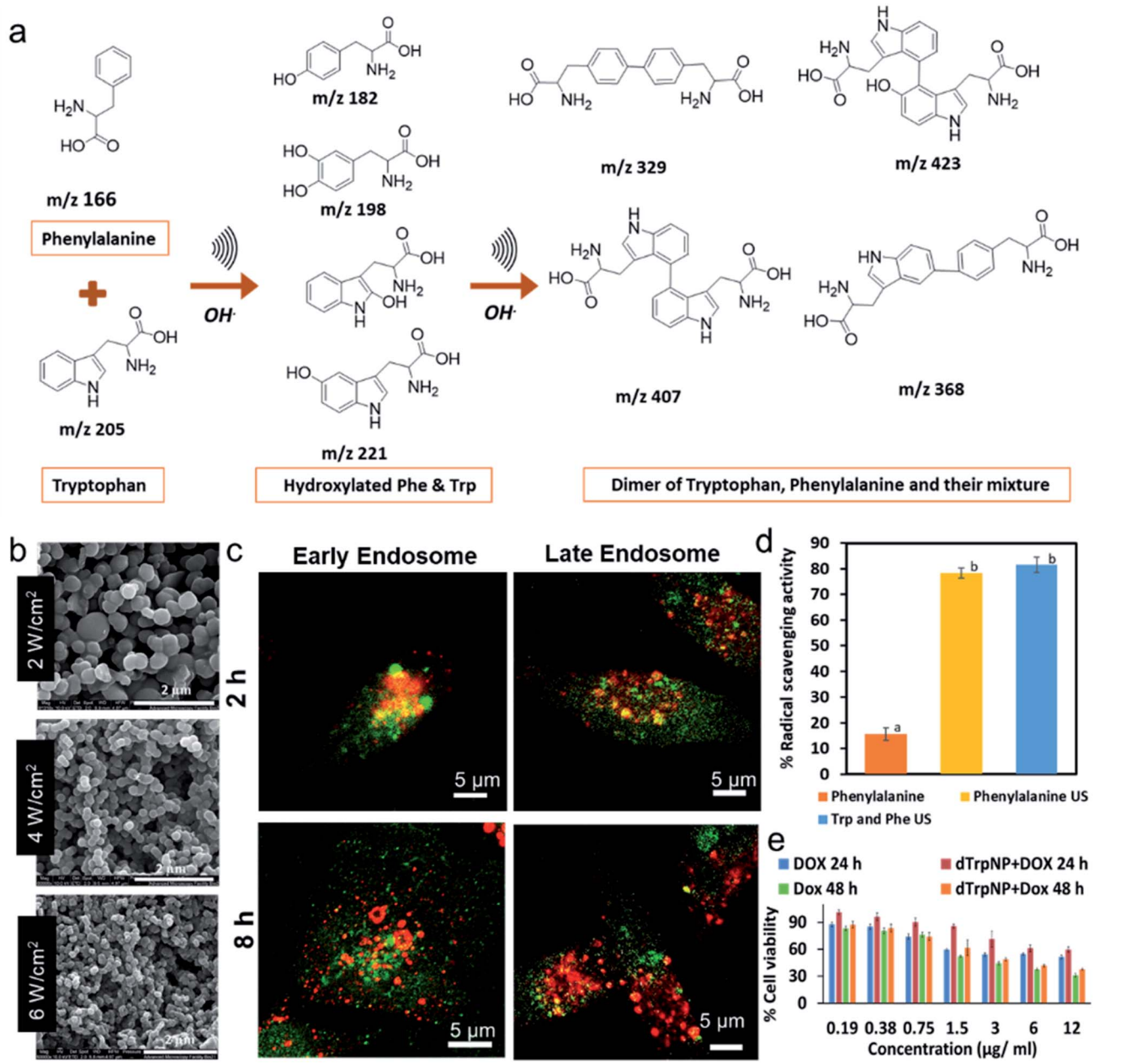

Fig. 2 (a) The schematic and proposed mechanism for the ultrasonic driven hydroxylation and dimerization of the phenylalanine and tryptophan, (b) SEM images phenylalanine nanoparticles obtained at 490 kHz at ultrasonic powers 2 W cm^{-1},² 4 W cm^{-2} and 6 W cm^{-2} respectively, (c) Confocal microscopy images of MDA-MB-231 cells incubated with tryptophan particles (green) for 2 h and 8 h and stained with early and late endosome (red) (d) The percentage DPPH radical scavenging of phenylalanine in comparison with sonicated phenylalanine and its mixture with tryptophan after 2 min incubation with DPPH solution and final concentration of 30 μg mL^{-1}. The significantly different values ($p < 0.05$) between the bars are denoted by alphabets. (e) Cell viability percentage of MDA-MB-231 cells after incubation with free doxorubicin and doxorubicin loaded on dTrpNP for 24 and 48 h.[32,33] ((c and e) – Adapted from ref. 33 with permission from The Royal Society of Chemistry.)

highly fluorescent nanoparticles from phenol. Most of the early studies focused only on the degradation of phenolic molecules using low frequency ultrasound.[35] Conversely, this study showed the formation of phenol dimers, trimers, and oligomers upon sonication at 355 kHz. Contrarywise, when the reaction was carried out at 20 kHz, no fluorescent dimers and oligomers were formed due to low OH radicals yield at this frequency. The oligomeric species further formed nanoaggregates by π–π which were found to have enhanced radical scavenging properties compared to phenol. Similarly, the sono-transformation of tannic acid into well-defined and controlled crystalline ellagic acid particles[29] has been reported. Tannic acid and ellagic acid are naturally occurring polyphenols with various applications in biomedicine and food.[36–38] The ellagic acid is mostly synthesized by enzymatic hydrolysis of the ellagitannins[39,40] or through multistep organic reactions[41] with poor control over size and its shape. In this study, high frequency ultrasound was utilized to perform multiple reactions to convert

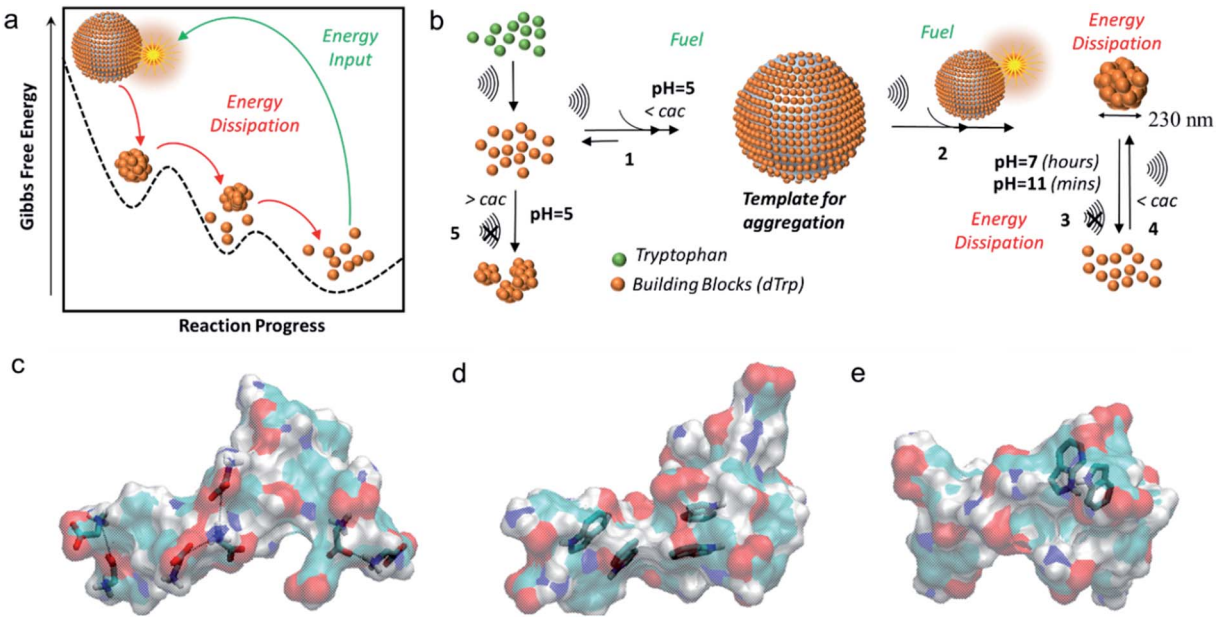

Fig. 3 (a) The Gibbs free energy diagram showing tryptophan dimers residing in global minimum and their dissipative self-assembly to tryptophan nanoparticles upon energy input provided by ultrasound and the tryptophan dimers recovering to their original state by energy dissipation; (b) general scheme for the ultrasound driven dissipative self-assembly of tryptophan dimers into nanoparticles; models of (c) ionic interactions, (d) $\pi-\pi$ interactions and (e) H-bond involving aromatic rings as acceptors. The tryptophan dimer molecules are shown as semi-transparent surfaces. The C, H, N and O atoms are colored in cyan, white, blue and red, respectively.[33] (Adapted from ref. 33 with permission from The Royal Society of Chemistry.)

tannic acid to ellagic acid particles-including hydrolysis of ester linkage, oxidative coupling of phenolic moieties and crystallization of product with controlled shape and size (Fig. 4a). Interestingly, the ultrasonic parameters were tuned to control the morphology of the ellagic micro-nanocrystals. The obtained particles exhibited different morphologies depending on the concentration of TA, frequency, power, and time of sonication. At specific ultrasonic time frequency and power, the size of the ellagic acid crystals surged from 3.7 to 7 μm with change in initial concentration of tannic acid solution from 0.5 mM (Fig. 4b) to 1 mM (Fig. 4c). By increasing the frequency from 355 kHz to 1 MHz at 5.5 W cm^{-3}, the size of the ellagic acid crystals was increased from 7 (Fig. 4c) to 9.5 microns (Fig. 4d) and the crystals morphology changed from ellipsoidal to discoidal. The increment in the sonication power from 5 W cm^{-3} to 20 W cm^{-3} at 355 kHz reduced the size from 7 μm to 270 nm (Fig. 4c, e–g). The change in frequency and power along with affecting the oxidation coupling process can also significantly affect the nucleation and growth kinetics during crystallisation which resulted in different size and morphology of the particles at various reaction and ultrasonic parameters. These particles showed promising and enhanced antioxidant and anticancer properties after 24 h incubation with MDA-MB-231 cells.

2.3 Ultrasound-driven assembly of synthetic peptides and proteins

It is widely reported that peptides can undergo several structural conformations to produce a broad range of nanostructures by self-assembly including nanofibers, spherical nanoparticles, nanotubes *etc.*[42–45] However, the control over self-assembling process is challenging and limited studies have reported peptide-based nanostructures with the controlled and well-defined morphologies.[46–48] Alves and coworkers[49,50] extensively studied a $[RF]_4$ octapeptide, which has arginine (R) and phenylalanine (F) in an alternating sequence. Their investigation confirmed that the octapeptide tends to form interconnected nanofibrillar structures rich in β-sheet structures, as well as other oligomeric species, by self-assembly *via* the solid-vapor phase method. Baral *et al.*[51] recently reported that high-frequency ultrasound can be used to control the crosslinking and self-assembly processes of the $[RF]_4$ octapeptide (Fig. 5a) to form well-defined fluorescent nanoparticles ($[RF]_4$–NPs), ~220 nm in diameter with ξ potential of +39 ± 6 mV (Fig. 5b).

The synthesized nanoparticles showed emission in blue, green, and red region as confirmed from the fluorescence microscopy images (Fig. 5c). Analysis of the sonication product at different sonication times by HPLC (Fig. 5d), confirmed that oxidative coupling led to the formation of high molecular weight species of $[RF]_4$ octapeptide. This was further supported by mass spectrometry results which suggested the coupling of the parent $[RF]_4$ octapeptides with [RF] and $[RF]_2$ fragments to form higher molecular weight species. $[RF]_4$–NPs were further functionalized with polyethylene glycol (PEGylated) to improve their colloidal stability, by preventing the aggregation tendency of $[RF]_4$–NPs. Unlike the parent peptide, the PEGylated $[RF]_4$–NPs showed limited cytotoxicity towards MDA-MB-231 cells (Fig. 5e) even at the concentration of 50 mg mL^{-1}. This was attributed to the fact that the peptide can form a layer over the

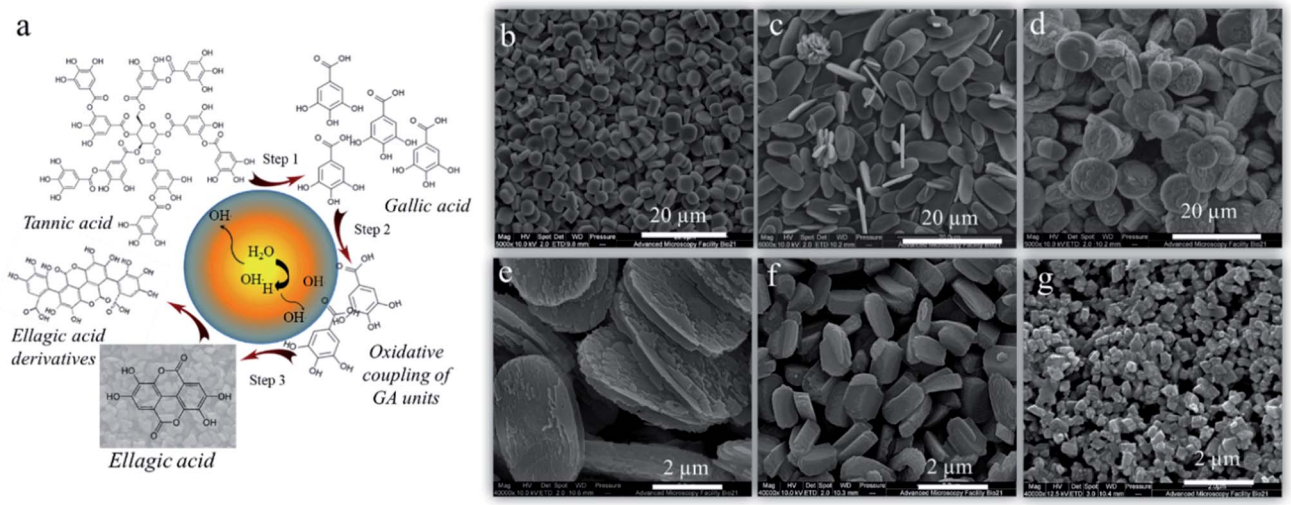

Fig. 4 (a) Schematic illustration of the mechanism of ultrasonic transformation of tannic to ellagic acid crystals, SEM images of the ellagic acid crystals produced after sonication of (b) 0.5 mM tannic acid at 355 kHz, 5.5 W cm^{-3}, (c) 1 mM tannic acid solution at 355 kHz, 5.5 W cm^{-3} (d) 1 mM tannic acid solution at 1058 kHz, 5.5 W cm^{-3}, (e), (f) and (g) 1 mM tannic acid solution at 355 kHz, 6.7 W cm^{-3}, 12 W cm^{-3} and 20 W cm^{-3} respectively.[29] (Reproduced from ref. 29 with permission from The Royal Society of Chemistry.)

cells which would lead to the disruption of the transmembrane activities[52] whereas the nanoparticles were uptaken by endocytosis. Moreover, the intracellular trafficking of PEGylated $[RF]_4$-NPs study with MDA-MB-231 cells showed effective *endo*-lysosomal escape (Fig. 5f) due to buffering capacity of the peptide nanoparticles in the *endo*-lysosomal vesicles pH range. This work highlighted that the combined use of sonochemistry and peptides can allow easy fabrication of nanoparticles, with potential application in nuclei acids and drug delivery.

Zhang *et al.*[53] first reported the synthesis of soy peptide nanoparticles (SPN) from large soy protein aggregates formed after proteolysis and thermal inactivation of soy protein isolates. The high intensity sonication (20 kHz) of large soy protein aggregates produced SPN of 100 nm with homogenous size distribution (PDI 0.20). Ultrasound induced molecular self-assembly by non-covalent interactions of insoluble peptide aggregates which resulted in the SPN formation and size of the nanoparticles was found to be dependent on the sonication time. To elucidate the interactions involved in the formation of nanoparticles, the effect of sodium dodecylsulfate (SDS), urea and dithiothreitol (DTT) on the formation of nanoparticles was analysed. The SDS, urea and DTT are known to disrupt hydrophobic interactions, hydrogen bonding and disulfide bonds, respectively.[54,55] It was reported that major intramolecular interactive forces responsible for maintaining the internal structure of nanoparticles were the hydrophobic interactions, whereas disulfide bonds played only minor role and hydrogen bonding was involved in the formation of their external structure. These SPN showed excellent emulsifying properties and antioxidant capacities when adsorbed on to oil droplets surface. In another similar study, after the proteolysis and hydrolysis, the soy peptide was sonicated to self-assemble through non-covalent interactions to fabricate core shell nanoparticles with homogenous particle size of ~104 nm (polydispersity index = 0.18).[56] The hydrophobic curcumin was then loaded to these nanoparticles which improved its shelf-life and water dispersity by 4 folds. Sono-assembled soy peptide nanoparticles were amenable to enzymatic degradation, showed enhanced bioavailability as well as controlled release of curcumin in the gastric-intestinal tract, which was demonstrated by *in vitro* studies. As these nanoparticles had remarkable radical oxygen species scavenging ability, they have been proposed as ingredients in functional food formulations. In another study, soy protein was used to modify the surface properties of bacterial cellulose (BC) electrospun nanofiber scaffold by ultrasound-induced self-assembly technique.[57] The modified nanofiber scaffold has multi-size distribution composed of BC electrospun nanofiber with diameter ranging from 80 to 360 nm and soy protein self-assembled nanoparticles on the surface, mimicking the structure of natural extracellular matrix. The as-prepared soy protein modified BC electrospun nanofiber scaffold was found bioactive as bone tissue engineering scaffold.

Liang *et al.*[58] demonstrated the effect of ultrasonic frequencies and other parameters on the synthesis of resveratrol-loaded zein particles. Particles exhibited a typical spherical shape with a diameter around 500 nm. The study revealed that the simultaneous use of triple frequency ultrasound (20/28/40 kHz) resulted in high encapsulation efficiency of resveratrol, attributed to a decrease in particle size and zeta potential of zein nanoparticles. Various forces including H-bonding, hydrophobic interactions and electrostatic interactions were involved in mechanism of formation of zein nanoparticles. Similarly, the effect of different multi-model frequency ultrasound treatment on the preparation of zein–chitosan complex coacervation for the encapsulation of resveratrol was reported.[59] Silk fibroin, a protein-based biomacromolecule with high biocompatibility, biodegradability, and low immunogenicity, was treated by highly intensified low frequency ultrasound (20 kHz) to obtain

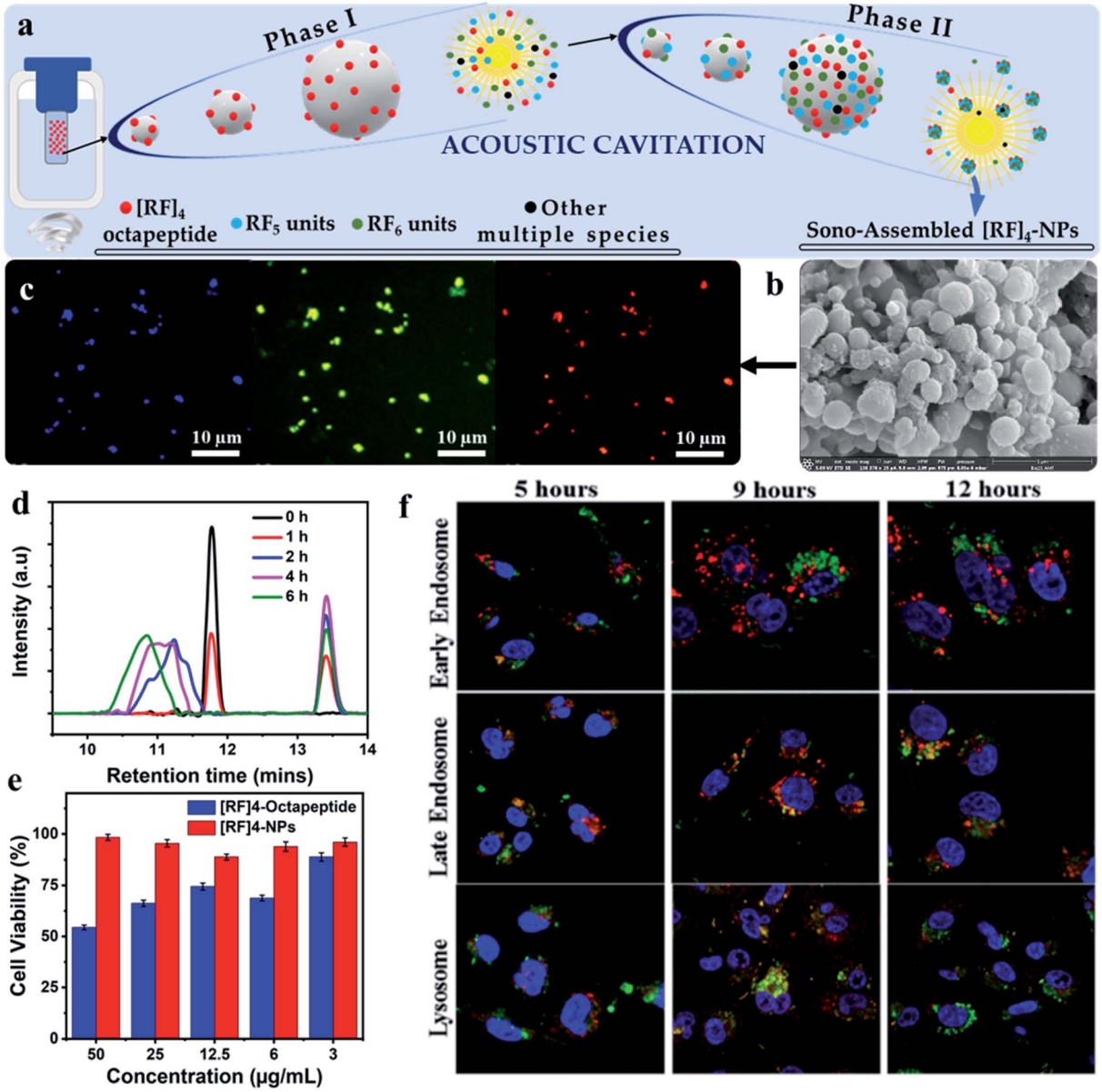

Fig. 5 Schematic depicting the (a) possible mechanism for the formation of different oligomeric species (phase I), which act as the fuel for fabricating highly fluorescent biofunctional sono-assembled $[RF]_4$–NPs under high frequency ultrasound, (b) SEM image of $[RF]_4$–NPs, (c) Fluorescence microscopy images of $[RF]_4$–NPs showing fluorescence in the blue, green and red region, formed by the oxidative coupling of $[RF]_4$ octapeptide into hydroxylated and high molecular weight species, (d) HPLC plot of the sonicated product suggesting the formation of hydroxylated and high molecular weight species, (e) cell viability performed on MDA-MB-231 cell line after 24 h incubation with using the [RF]4 octapeptide and $[RF]_4$–NPs, and (f) *endo*-lysosomal escape study of $[RF]_4$–NPs (green) with different intracellular vesicles (red) and cell nuclei (blue) after 5, 9 and 12 h of incubation time.[51]

nanoparticles. Silk fibroin was first sonicated to enhance the dissolution of the protein in ionic liquids, the mixture was then used to obtain the nanoparticles of size 180 ± 5 nm and zeta potential −25 mV using desolvation in polar organic solvents.[60,61] The synthesized nanoparticles showed high degree of β-sheet structure and minimal toxicity towards fibroblasts. These silk fibroin based nanoparticles, due to their excellent binding to various drugs and controlled drug release, have found applications in nanomedicine.[61]

In accordance with these studies, natural quinoa protein isolates were sonicated using low frequency ultrasound to improve the surface hydrophobicity of nanoparticles, as determined using contact angle measurements, and reduce the size of quinoa protein isolates from ~401 nm to ~207 nm.[62] The authors suggested that the nanoparticles can interact with each other by disulfide bonds and hydrophobic interactions and within 20 min of sonication, the interaction were altered to form smaller nanoparticles. The nanoparticles exhibited improved emulsification efficiency at concentrations above 1% w/v and stability when used to prepare biodegradable food-grade particle-based pickering emulsions, as compared to their native form. Another study by Zhang *et al.*[63] used

ultrasonicated fabricated quinoa protein nanoparticles (QPN) for the development of high internal phase emulsions (HIPES). The increased ultrasonic power density reduced the size of QPN to 132 nm (Fig. 6a) and improved its adsorption efficiency and antioxidant properties. The mechanism of stabilization and formation of QPN involved hydrophobic interactions and hydrogen bonding. The HIPES exhibited different microstructures for different QPN prepared at various power densities and were analyzed by interfacial tension measurements and confocal microscopy (Fig. 6b). The emulsion prepared with QPN synthesized at 1 kJ mL^{-1} acoustic power showed good flow behavior whereas the one prepare at 10 kJ mL^{-1} was firm (Fig. 6bI and II insets) due to the faster absorption kinetics towards oil-interface, as indicated from dynamic interfacial tension data (Fig. 6b I and II). Fig. 6b(III-VIII) suggest that power densities can also influence the size as well as the packing of the gel emulsion. In the HIPES obtained by using high power density QPN induced compressed droplets and formation of a polyhedral framework, furbishing the emulsion with viscoelasticity and pseudo-solid appearance. These QPN-stabilized HIPES could form a potential food ingredient in various emulsion-based products.

3. Summary and future outlook

In this review, we have presented a detailed overview of the sonochemical fabrication of nanostructures using low and high frequency ultrasound. Their formation mechanism, physicochemical properties, and potential applications primarily in biomedical and food areas were also discussed. So far, a range of biomolecules have been utilised including aromatic amino acids, polyphenols, peptides, and proteins. The synthesised nanoparticles in all the reported studies exhibited enhanced functional activities such as anticancer, antimicrobial, antioxidant activities and emulsifying properties compared to the parent biomolecules. Most importantly, the main advantages of ultrasound-based techniques in nanotechnology over conventional techniques are (i) the cavitation bubble surface acts as a microreactor and catalyst to perform reactions without resorting to any enzymes, metals, toxic organic solvents or synthetic catalyst, (ii) tailoring of nanoparticle size and morphology is achieved by the precise control over ultrasonic parameters, *viz.*, frequency, power, and sonication time. We can argue that this green and simple technology has the capability to process many biomolecules including natural compounds,

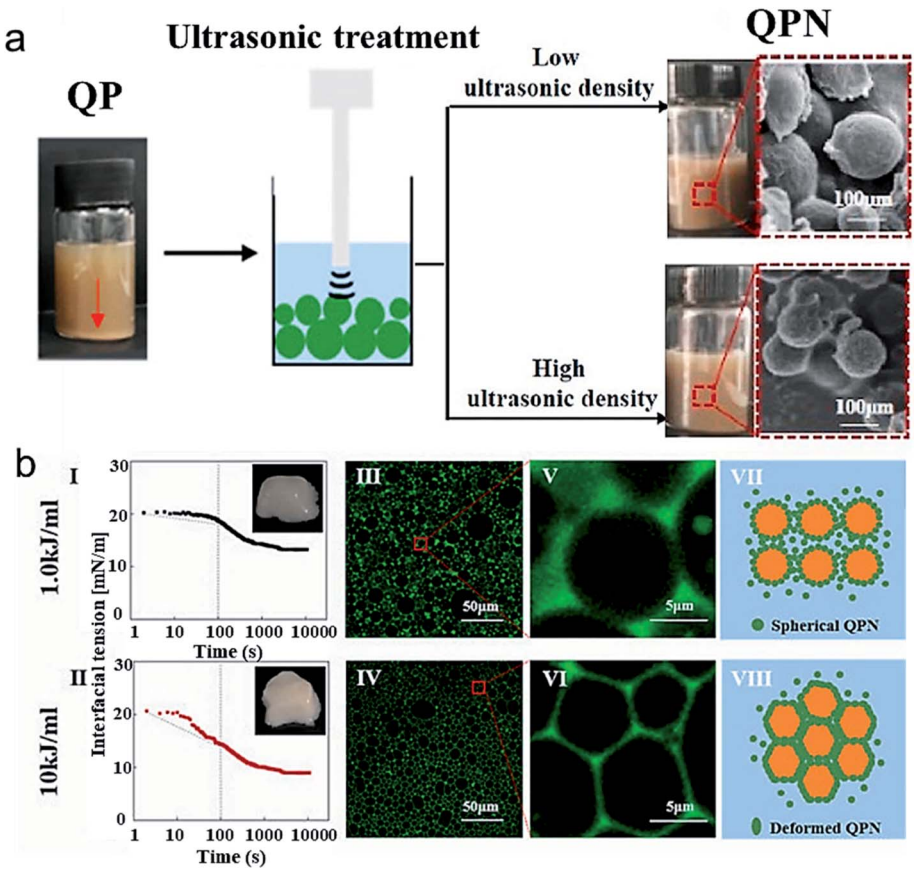

Fig. 6 (a) The scheme showing ultrasonication of QP at different power densities and its effect on the visual appearance and particle size of QPN when sonicated at low ultrasonic power density (1.0 kJ mol^{-1}) and high ultrasonic power density (10 kJ mol^{-1}) (b) (I and II) Dynamic interfacial tension as a function of time of fresh HIPEs stabilized by QPN prepared at 1.0 kJ mol^{-1} and 10 kJ mol^{-1} ultrasonic power density; (III–VI) Confocal laser scanning microscopy of the same fresh HIPEs and scheme illustrating the microstructure of HIPE stabilized by QPN synthesized at different power density QPN.[63] (Reproduced from ref. 63, Copyright (2021), with permission from Elsevier.)

antibiotics, anticancer drugs provided that the molecules bear sono-reactive chemical groups such as phenolic, quinone and aromatic groups. However, we cannot rule out that other possible reactions such as amidation, esterification, click chemistry reactions can take place at the reactive air-liquid interface of cavitation bubbles to obtain new nanomaterials. The sonication parameters, ionic strength, pH and concentration and the surface activity of biomolecules are key factors that collectively and synergistically play a role in the sound driven synthesis of nanomaterials. More studies are required to confirm and support the mechanisms of reaction involved in the formation of nanomaterials as well as various factors affecting the sonochemical reactivity of the biomolecules. In conclusion, we believe that the sound-driven methods for fabrication of nanoparticles have not been intensively studied therefore, the information covered in this minireview may help the research community to modify other types of biomolecules and obtain new nanoparticles with unprecedented properties.

Conflicts of interest

There are no conflicts to declare.

References

1 M. Elsabahy and K. L. Wooley, *Chem. Soc. Rev.*, 2012, **41**, 2545–2561.
2 S. D. Conner and S. L. Schmid, *Nature*, 2003, **422**, 37–44.
3 F. Zhao, Y. Zhao, Y. Liu, X. Chang, C. Chen and Y. Zhao, *Small*, 2011, **7**, 1322–1337.
4 A. Verma and F. Stellacci, *Small*, 2010, **6**, 12–21.
5 V. P. Torchilin, *AAPS J.*, 2007, **9**, E128–E147.
6 B. Simionescu and D. Ivanov, *Handbook of Bioceramics and Biocomposites*, Springer, 2016, pp. 233–286.
7 A. R. Wassel, M. E. El-Naggar and K. Shoueir, *J. Environ. Chem. Eng.*, 2020, **8**, 104175.
8 S. Sur, A. Rathore, V. Dave, K. R. Reddy, R. S. Chouhan and V. Sadhu, *Nano-Struct. Nano-Objects*, 2019, **20**, 100397.
9 S. D. Anderson, V. V. Gwenin and C. D. Gwenin, *Nanoscale Res. Lett.*, 2019, **14**, 188.
10 C. Dhand, N. Dwivedi, X. J. Loh, A. N. J. Ying, N. K. Verma, R. W. Beuerman, R. Lakshminarayanan and S. Ramakrishna, *RSC Adv.*, 2015, **5**, 105003–105037.
11 B. Banerjee, *Ultrason. Sonochem.*, 2017, **35**, 1–14.
12 S. K. Bhangu and M. Ashokkumar, Theory of Sonochemistry, in *Topics in Current Chemistry Collections*, ed. J. Colmenares, G. Chatel, Springer, 2017, pp. 1–28.
13 K. Okitsu and Y. Nunota, *Ultrason. Sonochem.*, 2014, **21**, 1928–1932.
14 S. Aashima, S. K. Pandey, S. Singh and S. K. Mehta, *Ultrason. Sonochem.*, 2018, **49**, 53–62.
15 L. Lee, F. Cavalieri and M. Ashokkumar, *Langmuir*, 2019, **35**, 9997–10006.
16 H. Zhu, S. Mettu, M. A. Rahim, F. Cavalieri and M. Ashokkumar, *Food Chem.*, 2021, 130236.
17 Y. Mizukoshi, K. Okitsu, Y. Maeda, T. A. Yamamoto, R. Oshima and Y. Nagata, *J. Phys. Chem. B*, 1997, **101**, 7033–7037.
18 M. Ashokkumar, in *Ultrasonic Synthesis of Functional Materials*, Springer, 2016, pp. 17–40.
19 T. Leong, M. Ashokkumar and S. Kentish, *Acoust. Aust.*, 2011, **39**, 54–63.
20 N. S. Yusof, B. Babgi, Y. Alghamdi, M. Aksu, J. Madhavan and M. Ashokkumar, *Ultrason. Sonochem.*, 2016, **29**, 568–576.
21 M. A. Beckett and I. Hua, *J. Phys. Chem. A*, 2001, **105**, 3796–3802.
22 M. Capocelli, E. Joyce, A. Lancia, T. J. Mason, D. Musmarra and M. Prisciandaro, *Chem. Eng. J.*, 2012, **210**, 9–17.
23 P. Kanthale, M. Ashokkumar and F. Grieser, *Ultrason. Sonochem.*, 2008, **15**, 143–150.
24 C. Petrier, A. Jeunet, J. L. Luche and G. Reverdy, *J. Am. Chem. Soc.*, 1992, **114**, 3148–3150.
25 K. S. Suslick and L. A. Crum, *Sonochemistry and Sonoluminescence*, Wiley-Interscience, New York, 1998.
26 H. Zhu, F. Cavalieri and M. Ashokkumar, *Macromol. Chem. Phys.*, 2018, **219**, 1800353.
27 Z. L. Gao, H. Y. Zhu, X. Y. Li, P. Y. Zhang, M. Ashokkumar, F. Cavalieri, J. C. Hao and J. W. Cui, *ACS Macro Lett.*, 2019, **8**, 1285–1290.
28 H. Zhu, S. Mettu, F. Cavalieri and M. Ashokkumar, *Food Chem.*, 2021, **353**, 129432.
29 S. K. Bhangu, R. Singla, E. Colombo, M. Ashokkumar and F. Cavalieri, *Green Chem.*, 2018, **20**, 816–821.
30 C. Petrier, A. Jeunet, J. L. Luche and G. Reverdy, *J. Am. Chem. Soc.*, 1992, **114**, 3148–3150.
31 F. Cavalieri, E. Colombo, E. Nicolai, N. Rosato and M. Ashokkumar, *Mater. Horiz.*, 2016, **3**, 563–567.
32 S. K. Bhangu, M. Ashokkumar and F. Cavalieri, *Ultrason. Sonochem.*, 2020, **63**, 104967.
33 S. K. Bhangu, G. Bocchinfuso, M. Ashokkumar and F. Cavalieri, *Nanoscale Horiz.*, 2020, **5**, 553–563.
34 S. K. Bhangu, M. Ashokkumar and F. Cavalieri, *ACS Sustainable Chem. Eng.*, 2017, **5**, 6081–6089.
35 C. Wu, X. Liu, D. Wei, J. Fan and L. Wang, *Water Res.*, 2001, **35**, 3927–3933.
36 H. Ejima, J. J. Richardson, K. Liang, J. P. Best, M. P. van Koeverden, G. K. Such, J. Cui and F. Caruso, *Science*, 2013, **341**, 154–157.
37 S. Quideau, D. Deffieux, C. Douat-Casassus and L. Pouysegu, *Angew. Chem., Int. Ed. Engl.*, 2011, **50**, 586–621.
38 N. Bertleff-Zieschang, M. A. Rahim, Y. Ju, J. A. Braunger, T. Suma, Y. Dai, S. Pan, F. Cavalieri and F. Caruso, *Chem. Commun.*, 2017, **53**, 1068–1071.
39 A. Brune and B. Schink, *Arch. Microbiol.*, 1992, **157**, 417–424.
40 L. Mingshu, Y. Kai, H. Qiang and J. Dongying, *J. Basic Microbiol.*, 2006, **46**, 68–84.
41 Q. Sun, J. Heilmann and B. König, *Beilstein J. Org. Chem.*, 2015, **11**, 249.
42 M. Zelzer and R. V. Ulijn, *Chem. Soc. Rev.*, 2010, **39**, 3351–3357.
43 J. Castillo-León, K. B. Andersen and W. E. Svendsen, *ACS Biomater. Sci. Eng.*, 2011, 115–138.

44 S. Zhang, T. Holmes, C. Lockshin and A. Rich, *Proc. Natl. Acad. Sci. U. S. A.*, 1993, **90**, 3334–3338.
45 Y. Zhao, W. Yang, C. Chen, J. Wang, L. Zhang and H. Xu, *Curr. Opin. Colloid Interface Sci.*, 2018, **35**, 112–123.
46 B. K. Shanbhag, C. Liu, V. S. Haritos and L. Z. He, *ACS Nano*, 2018, **12**, 6956–6967.
47 M. A. Greenfield, J. R. Hoffman, M. Olvera de la Cruz and S. I. Stupp, *Langmuir*, 2009, **26**, 3641–3647.
48 Y. Kuang, Y. Gao, J. Shi, H. C. Lin and B. Xu, *Chem. Commun.*, 2011, **47**, 8772–8774.
49 C. C. Decandio, E. R. Silva, I. W. Hamley, V. Castelletto, M. S. Liberato, V. X. Oliveira, C. L. Oliveira and W. A. Alves, *Langmuir*, 2015, **31**, 4513–4523.
50 M. S. Liberato, S. Kogikoski, E. R. Silva, M. D. Coutinho-Neto, L. P. Scott, R. H. Silva, V. X. Oliveira Jr, R. m. A. Ando and W. A. Alves, *J. Phys. Chem. B*, 2013, **117**, 733–740.
51 A. Baral, S. K. Bhangu, R. Cimino, J. Pelin, W. A. Alves, S. Chattopadhyay, M. Ashokkumar and F. Cavalieri, *Nanomaterials*, 2020, **10**, 1772.
52 N. J. Yang and M. J. Hinner, *Methods Mol. Biol.*, 2015, **1266**, 29–53.
53 Y. H. Zhang, F. B. Zhou, M. M. Zhao, L. Z. Lin, Z. X. Ning and B. G. Sun, *Food Hydrocolloids*, 2018, **74**, 62–71.
54 N. Chen, L. Lin, W. Sun and M. Zhao, *J. Agric. Food Chem.*, 2014, **62**, 9553–9561.
55 K. S. Liu and F. H. Hsieh, *J. Am. Oil Chem. Soc.*, 2007, **84**, 741–748.
56 Y. Zhang, M. Zhao, Z. Ning, S. Yu, N. Tang and F. Zhou, *J. Agric. Food Chem.*, 2018, **66**, 4208–4218.
57 C. Zhijiang, X. Ping, H. Shiqi and Z. Cong, *Cellulose*, 2019, **26**, 6133–6150.
58 Q. F. Liang, X. F. Ren, X. Zhang, T. Hou, M. Chalamaiah, H. L. Ma and B. Xu, *J. Food Eng.*, 2018, **221**, 88–94.
59 X. Ren, T. Hou, Q. Liang, X. Zhang, D. Hu, B. Xu, X. Chen, M. Chalamaiah and H. Ma, *Food Chem.*, 2019, **279**, 223–230.
60 A. A. Lozano-Pérez, M. G. Montalbán, S. D. Aznar-Cervantes, F. Cragnolini, J. L. Cenis and G. Víllora, *J. Appl. Polym. Sci.*, 2015, 132.
61 Z. Zhao, Y. Li and M. B. Xie, *Int. J. Mol. Sci.*, 2015, **16**, 4880–4903.
62 X. S. Qin, Z. G. Luo and X. C. Peng, *J. Agric. Food Chem.*, 2018, **66**, 4449–4457.
63 X. X. Zhang, Z. Y. Zuo, W. J. Ma, P. B. Yu, T. Li and L. Wang, *Food Hydrocolloids*, 2021, **117**, 106748.